

Stereochemical Strategy Advances Microbially Antiadhesive Cotton Textile in Safeguarding Skin Flora

Jiangqi Xu, Hongjuan Zhao, Zixu Xie, Scott Ruppel, Xiaqing Zhou, Shuang Chen, Jun F. Liang, and Xing Wang*

Microbial contamination on cotton textiles (CT) negatively affects people's health as well as the textile itself during use and storage. Using antimicrobial CT in a body-safe manner is currently still a challenge because it is difficult to balance killing microbes and protecting skin flora. Herein, a borneol-decorated CT (BDCT) through coupling of borneol 4-formylbenzoate molecules onto the amino-modified CT is reported. This BDCT shows strong and broad-spectrum microbially antiadhesive activities against gram-positive bacteria (*Staphylococcus aureus* and *S. epidermidis*), gram-negative bacteria (*Escherichia coli* and *Pseudomonas aeruginosa*), and fungi (*Aspergillus niger*, *Mucor racemosus*, and *Candida albicans*). Because of its unique stereochemical microbial antiadhesion mechanism, BDCT is harmless to skin flora. In addition, BDCT exhibits prominent durability of microbially antiadhesive capability by bearing 50 times of accelerated laundering. Therefore, this stereochemical BDCT strategy shows great potential for applications in the new generation of textiles, food packaging, and medical protection.

antimicrobial CT is desired.^[2] Nowadays, antimicrobial CT can be obtained through introducing various kinds of antimicrobial agents,^[3] such as antibiotics,^[4] metals and metal salts,^[5,6] quaternary ammonium,^[7] and some specific molecules.^[8–11] Although those modified textiles showed good antibacterial activities, killing microorganisms usually when they come into contact with material surfaces,^[3,12] the shortcomings are also obvious by their toxicity, narrow spectrum, resistance, and damage to skin flora. For example, triclosan had been used in textiles widely,^[12,13] but now it has been banned by many countries because of its accessory substance of toxic polychlorinated dioxins.^[14,15] Besides, killing strategies caused the dead microbes which still contaminate material surfaces and the residues not only degrade biocides' activity but also provide nutrients for other colonizers.^[16] Furthermore, the dead micro-

1. Introduction

Cotton textiles (CT) are widely used in daily life. However, it also provides perfect culture environment for microorganisms that realistically threaten the health of human beings.^[1] Microbial contamination in hospitals such as on gloves, masks, and gowns is known to be the major source of cross infection. With increasing awareness of health and hygiene for consumers,

bial structures could still contain active allergenic compounds to humans. Also, the biocides can impact skin flora,^[17] which is originally beneficial to human health.^[18] Once the microecological balance of human skin is broken, pathogenic bacteria would have opportunity to invade. Therefore, there is a strong demand for making antimicrobial CT more safety especially on protecting skin flora.

Microbial antiadhesion may offer a solution for safe use of antimicrobial CT because the nonkilling property could reduce the harm to human skin flora.^[17] In the field of bacterially antiadhesive CT, only a few literatures focused on it. For example, Chen et al. developed a series of antimicrobial and antifouling cotton fabrics via dually finished with quaternary ammonium salt and zwitterionic sulfobetaine with laundering stability.^[2,19,20] The hydrophilicity of zwitterions endowed the cotton fabrics with effective bacterial antiadhesion, hydrophilicity, and moisture permeability. Lin et al. designed antibacterial and bacterially antiadhesive cotton fabrics coated by cationic fluorinated polymers. These cotton fabrics achieved bacterial antiadhesion mainly by hydrophobicity.^[21] Sivakumar et al. developed a chalcone coating on cotton cloth to reduce bacterial adhesion.^[22] As an alternative, we recently developed a soft "surface stereochemistry" strategy, on the basis of a well-accepted theory that cells could distinguish molecular chirality,^[23,24] to regulate microbial reversible adhesion in the

J. Xu, H. Zhao, Z. Xie, Prof. X. Wang
Beijing Advanced Innovation Center for Soft Matter Science and Engineering
Beijing Laboratory of Biomedical Materials
Beijing University of Chemical Technology
Beijing 100029, P. R. China
E-mail: wangxing@mail.buct.edu.cn

S. Ruppel, X. Zhou, S. Chen, Prof. J. F. Liang, Prof. X. Wang
Department of Biomedical Engineering, Chemistry, and Biological Sciences
Charles V. Schaefer School of Engineering and Sciences
Stevens Institute of Technology
Hoboken, NJ 07030, USA

 The ORCID identification number(s) for the author(s) of this article can be found under <https://doi.org/10.1002/adhm.201900232>.

DOI: 10.1002/adhm.201900232

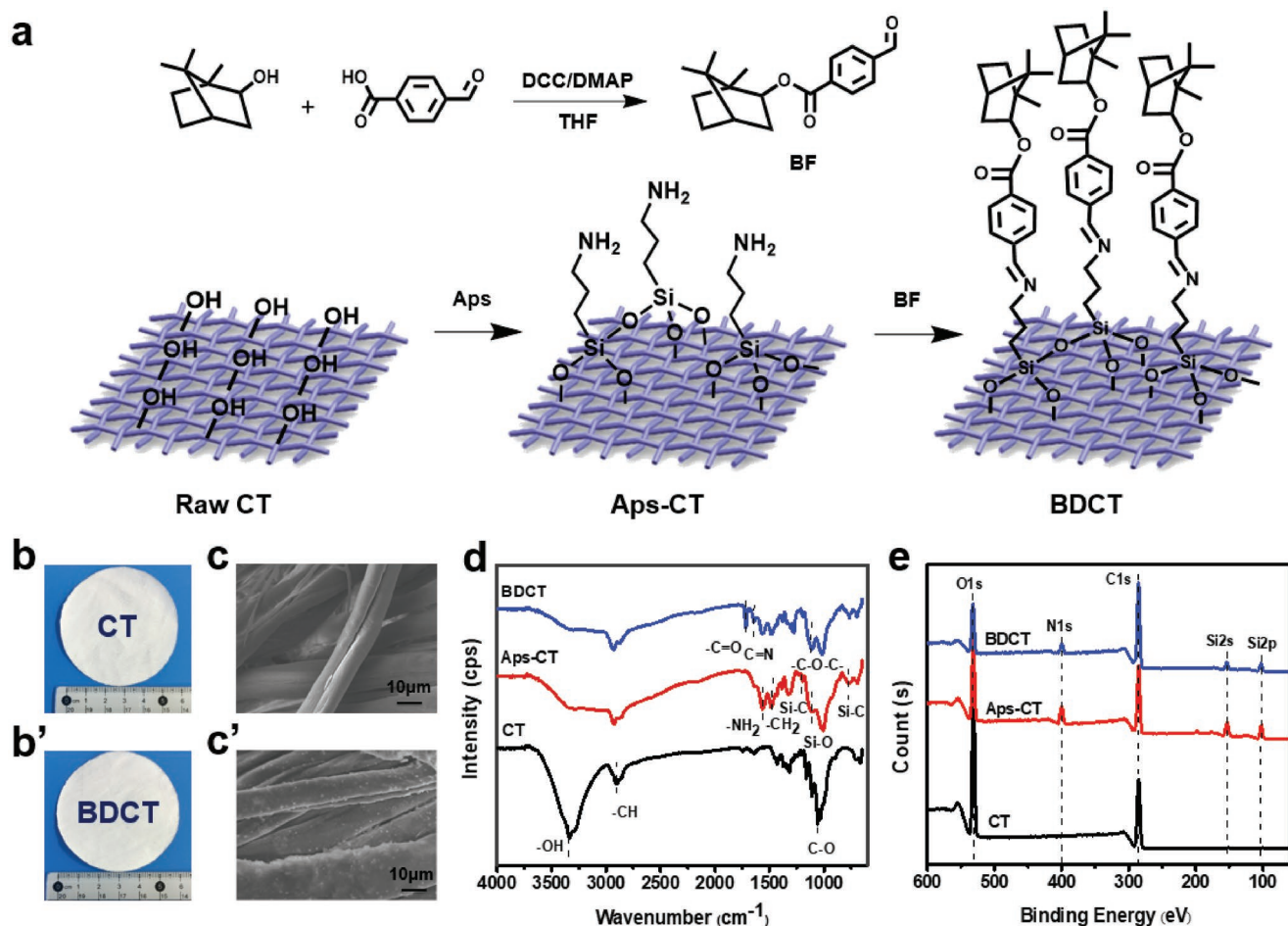


Figure 1. a) Schematic illustration of the decorating processes of BDCT. b, b') Digital photos of raw CT and BDCT. c, c') SEM images of raw CT and BDCT. d) ATR-FTIR and e) XPS spectra of BDCT (top), Aps-CT (middle), and raw CT (bottom).

initial stage of microbe–material interaction.^[25,26] This strategy employed the chiral borneol-based polymers that can control microbial contamination through influencing their “chiral taste.”^[27,28] Besides safety and biocompatibility, the unique feature of the polymers is effectively antimicrobial adhesion other than killing microbes. These properties are well suited for CT decoration. We thus foresee that controlling microbial adhesion but not killing microbes could be useful and highlighted on protecting skin flora.

Herein, we present a facile design of borneol-decorated CT (BDCT) via Schiff-base coupling (Figure 1a) of borneol 4-formylbenzoate (BF) molecules onto the 3-aminopropyltrimethoxysilane-modified CT (Aps-CT), where the big hydrophobic borneol group could strongly stabilize the Schiff-base bond.^[29–31] The broad-spectrum microbially antiadhesive activities and microbially antiadhesive durability of BDCT against gram-positive bacteria *Staphylococcus aureus* (*S. aureus*) and *Staphylococcus epidermidis* (*S. epidermidis*), gram-negative bacteria *Escherichia coli* (*E. coli*) and *Pseudomonas aeruginosa* (*P. aeruginosa*), and fungi *Aspergillus niger* (*A. niger*), *Mucor racemosus* (*M. racemosus*), and *Candida albicans* (*C. albicans*) were investigated. In particular, the effects on skin flora and skin stimulation were studied.

2. Results and Discussion

2.1. Synthesis and Characterization of BDCT

The decorating process involved covalent bonding of Aps on CT and then surface Schiff-base coupling of BF (Figure 1a). The reaction conditions were mild. Aps acted as an effective linker, endowing CT with amino-terminal and further bonding BF molecules on it. BDCT maintained the appearance of the pristine CT (Figure 1b, b'), where the whiteness of the fabrics basically remain unchanged (CT: 85.80; BDCT: 85.35). But the scanning electron microscope (SEM) image of BDCT showed a granulated thin film on it, rougher than that of raw CT (Figure 1c, c'). This phenomenon confirmed the decorating process. The degree of grafting (DG) of BDCT was 14.6%.

Figure 1d presents the attenuated total reflection Fourier transformed infrared (ATR-FTIR) spectra of BDCT and the control groups. First, all the samples were characterized with dominant O–H stretching vibration (3070–3570 cm^{-1}), C–H stretching vibration (2805–3000 cm^{-1}), and C–O stretching vibration (1029 cm^{-1}) because of the presence of basic glucose units. For Aps-CT, the bands of characteristic –NH_2 (1569 cm^{-1}) and –CH_2 (1483 cm^{-1}) stretching vibrations were displayed

in the spectrum. Meanwhile, the band at 1100 cm^{-1} was characteristic stretching vibration of Si–O; the bands at 760 and 1200 cm^{-1} were assigned to Si–C. These bands were not observed in raw CT, indicating the grafting of Aps on CT. As a result, the O–H stretching vibration peaked at 3300 cm^{-1} was decreased clearly. After coupling with BF, the sample showed characteristic peaks of ester at 1722 cm^{-1} for C=O and Schiff base at 1636 cm^{-1} for C=N, respectively, confirming the successful synthesis of BDCT.

More evidence was supplied by X-ray photoelectron spectroscopy (XPS) detection (Figure 1e). Only the characteristic signals of C1s and O1s were observed at the surface of raw CT. Signals of N1s and Si2p were detected for Aps-CT, and the N/Si atomic ratio was 1.1, which was very close to the theoretical value. When BF was grafted, the signal of C1s was enhanced obviously. The C/O ratio of BDCT (C: 72.13 at%, O: 16.64 at%) was increased to 4.33 compared with the ratio of 1.40 of raw CT (C: 58.42 at%, O: 41.85 at%), confirming the decorating of borneol C_{10} groups. To further confirm the details, we analyzed the composition of C, N, and O elements. As shown in Figure S1a (Supporting Information), the C1s spectrum of raw CT was three deconvoluted peaks located at 283.4, 284.8, and 286.3 eV, corresponding to carbon atoms in C–C/C–H, C–O, and O–C–O, respectively. While for BDCT, the C1s spectrum (Figure S1a', Supporting Information) showed a new peak associated with C=O bond (288.8 eV) of BF. A deconvoluted peak located at 286.2 eV can be attributed to C=N bond. Figure S1b (Supporting Information) displays the N1s spectrum of Aps-CT at 400.1 eV that represents $-\text{NH}_2$ groups. While Figure S1b' (Supporting Information) of BDCT shifted its N1s spectra to a lower energy at 398.9 eV, which is attributed to the Schiff-base coupling of C=N. Figure S1c,c' (Supporting Information) showed the O1s spectra. The peak shift from 531.4 eV (O–H and O–C) to 532.2 eV (O–Si and O=C–O) also suggested the final modification of BDCT.

2.2. Bacterially Antiadhesive Capability

The bacterially antiadhesive activities of BDCT were quantitatively evaluated using viable cell count method^[32] against Gram-negative bacteria (*E. coli* and *P. aeruginosa*) and Gram-positive bacteria (*S. aureus* and *S. epidermidis*). Typically, *E. coli* and *S. aureus* are commonly used strains for bacterially antiadhesive evaluation; *P. aeruginosa* is a common bacterium that causes wound infection; *S. epidermidis* grows on the epidermis of living organisms that belongs to the normal flora of human skin. As shown in Figure 2a, bacterial adhesion on BDCT against *E. coli*, *P. aeruginosa*, *S. aureus*, and *S. epidermidis* totally showed a distinct reduction, when compared with that on raw CT. Figure 2b quantified the number of bacterial adhesion on CT and BDCT. Bacterial adhesion number of BDCT was significantly less than that of CT for each bacteria type ($p < 0.001$). The \log_{10} reduction in bacterial adhesion count of BDCT is shown in Figure S2 (Supporting Information). BDCT resulted in a 1.47 \log_{10} , 1.36 \log_{10} , 2.94 \log_{10} , and 2.90 \log_{10} (CFU mL^{-1}) reduction in bacterial adhesion count of *E. coli*, *P. aeruginosa*, *S. aureus*, and *S. epidermidis*, respectively. The results indicated that BDCT had excellent bacterially antiadhesive activities against broad-spectrum bacteria.

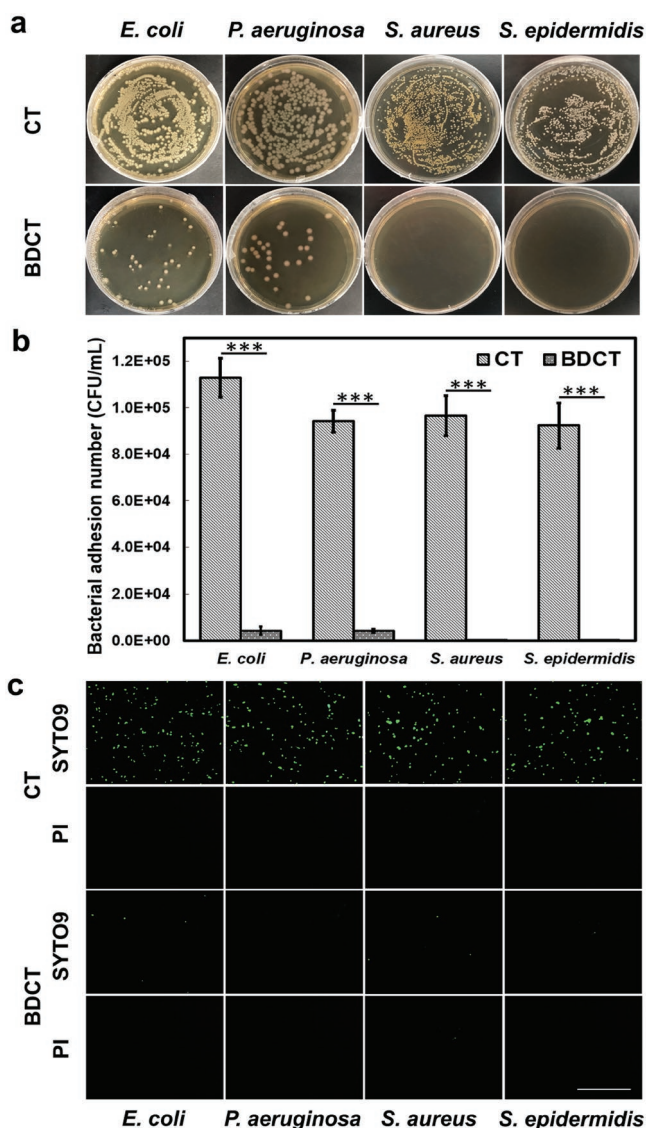


Figure 2. a) Bacterial antiadhesion of raw control CT and BDCT against *E. coli*, *P. aeruginosa*, *S. aureus*, and *S. epidermidis*. b) Bacterial adhesion number (CFU mL^{-1}) on CT and BDCT. Data presented as mean \pm SD, $n = 3$. Two-tailed t -test; ***represents $p < 0.001$. c) BacLight live/dead fluorescent assay of bacteria adhered to raw control CT and BDCT. The scale bar in the image is $20\text{ }\mu\text{m}$.

Meanwhile, bacteria that adhered to BDCT and raw control CT were investigated through the BacLight live/dead fluorescent assay.^[26] The bacterial population (green fluorescence of SYTO9 staining in Figure 2c) on the surface of BDCT reduced dramatically compared with that on the raw CT. There were no dead bacteria (red fluorescence of PI staining in Figure 2c) found on the surface of BDCT and the raw CT. This result proved the above speculation, where BDCT could inhibit bacterial adhesion instead of killing bacteria. BDCT would not do harm to normal skin flora, such as *S. epidermidis*, while could resist environmental pathogenic bacterial contamination, such as *P. aeruginosa*, which could cause various types of infections.

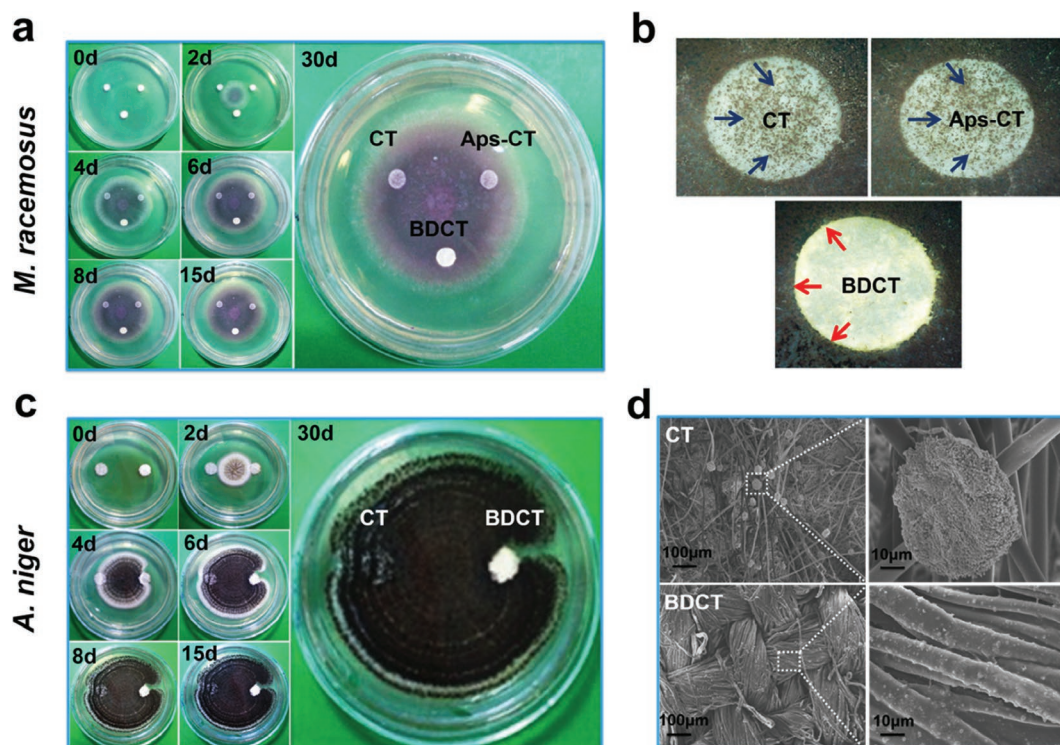


Figure 3. a) Fungal antiadhesion of raw CT (left), Aps-CT (right), and BDCT (bottom) by culturing *M. racemosus* in the center location of solid medium, in the same plate for different periods (0, 2, 4, 6, 8, 15, and 30 d). b) Enlarged images of CT, Aps-CT, and BDCT cultured with *M. racemosus* for 30 d. c) Fungal antiadhesion of raw CT (left) and BDCT (right) by culturing *A. niger* in the center location of solid medium, in the same plate for different periods (0, 2, 4, 6, 8, 15, and 30 d). d) SEM images of fungally antiadhesive results on raw CT and BDCT surfaces. Left are images at low magnifications; right are images at high magnifications.

2.3. Fungally Antiadhesive Assay

To intuitively demonstrate the fungally antiadhesive capability of BDCT, we performed the “invasion experiment” with *M. racemosus*, *A. niger*, and *C. albicans*.^[27] As shown in **Figure 3a**, raw CT, Aps-CT, and BDCT pellets were put into the same plate with solid medium, culturing *M. racemosus* in the center location. A drop of fungi grew and expanded from center to the border. After 2 d of incubation, *M. racemosus* grew to the edge of pellets and started to attack the samples. A significant difference was observed after 4 d of incubation. The raw CT and Aps-CT pellet were gradually covered with *M. racemosus*, as the conidia could be visualized on the surface; but on the BDCT surface, no fungal cells adhered or grew on it. Those microbes bypassed the BDCT pellet, or in other words, the BDCT pellet stopped the growth and expansion of *M. racemosus* on it. After 6 d, *M. racemosus* covered almost entirely the raw CT and Aps-CT pellets, meaning the raw CT and Aps-CT did not inhibit fungal growth. In contrast, even after 30 d, the BDCT sample exhibited a clear surface without any fungal stains (**Figure 3b**), thus demonstrating the ability to inhibit adhesion and growth of *M. racemosus*.

Beyond this, another fungus, *A. niger*, was also used to conduct the invasion experiment to evaluate the broad fungally antiadhesive spectrum of BDCT. As shown in **Figure 3c**, the positive result was obtained. A clear surface with a distinct boundary was found for BDCT even after 30 d incubation,

demonstrating its remarkable performance on antiadhesion of *A. niger*. SEM measurements were also used to detect microphenomena on the surface of the samples. **Figure 3d** showed the interactions and morphologies of fungal cells adhered on the above-mentioned pellets. Numerous sporangia and hypha were found on raw CT surface, and lively germination of spores was exhibited in a magnified image. In contrast, on the surface of BDCT, no hypha and no spores, only the decorated cotton fibers could be observed. According to this phenomenon, BDCT mainly performed a defensive effect on fungal adhesion. Meanwhile, there were also no dead or fragmented fungal cells around or on BDCT. That is, the BDCT sample can maintain a balanced state with the surrounding flora. It stopped fungal invasion but did not kill them. Therefore, for skin ecological environment, we deduced that BDCT would not do harm to skin flora even at close contact, while might resist environmental fungal contamination effectively. Moreover, BDCT could hold its fungally antiadhesive properties even after four repeated challenges against *A. niger* every 4 d of intervals (**Figure S3**, Supporting Information).

Additionally, BDCT can also inhibit the growth and adhesion of human pathogenic fungus *C. albicans*. As shown in **Figure S4** (Supporting Information), after 10 d of incubation, *C. albicans* could grow onto raw CT and Aps-CT surface; however, it did not grow onto the BDCT surface. The BDCT showed a distinct boundary against *C. albicans*.

2.4. Skin Flora Evaluation

Skin flora contributes to an important barrier for protecting human body from harmful microbial invasion.^[33] The use of antimicrobial clothes has raised issues concerning skin health.^[17] Therefore, the interaction between skin flora and BDCT is important. Skin flora evaluation was thus designed according to the national standard (GB/T 31713-2015). Guinea pigs were used in this experiment as alternatives to human skins.^[34] The animal experimental model is shown in Figure 4a. As shown in Figure 4b, whether before or after dressing BDCT, the bacterial species showed no difference. The bacteria detected from the skin before and after contacting BDCT were identified according to their 16S rDNA sequence

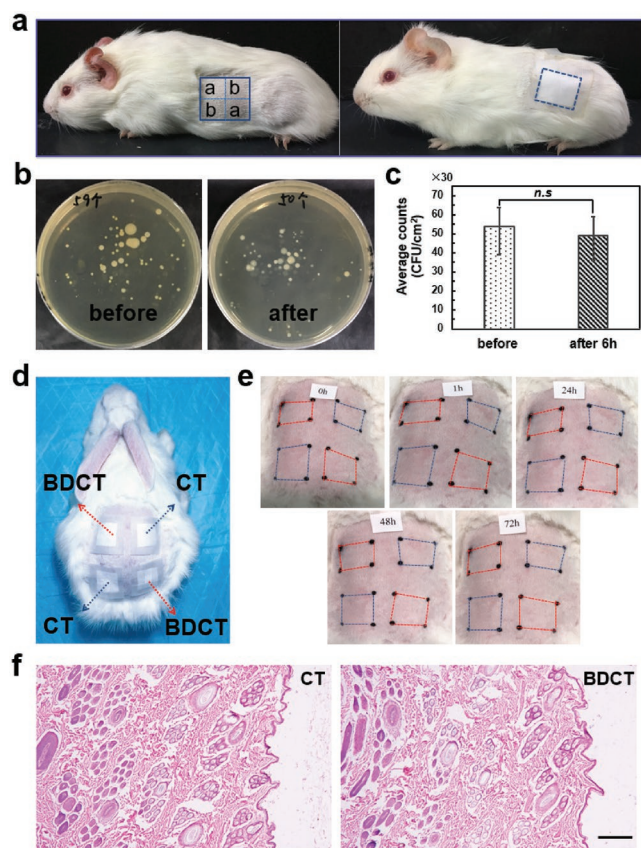


Figure 4. a) Model of skin flora test: Guinea pig in the left picture showed the application site to cover the sample (in the circle marked with blue line). The region “a” was the area where bacteria were taken from before coating samples. The region “b” was the area where bacteria were taken from after coating the samples. The right picture showed guinea pig in contact with the BDCT. b) The culturing results of bacterial flora of guinea pig skin before and after applying BDCT. c) Average of total germ counts (CFUs cm⁻²) of guinea pig skin before and after the application of BDCT. Data presented as mean ± SD, $n = 30$. Statistical analysis was performed using Student’s *t*-test to test the significance of differences. n.s. represents $p > 0.05$. d) Model of animal skin irritation according to ISO 10993-10:2010 standard. e) The images are rabbits’ back contacting BDCT (in the circles marked with red-dotted lines) and negative control (in the circles marked with blue-dotted lines) at 0, 1, 24, 48, and 72 h. f) Histopathological analysis of skin with H&E staining of skin contacted with CT and BDCT at 72 h. The scale bar is 200 μm.

analysis. The results indicated that the bacteria were mainly *Acinetobacter* sp. Figure 4c shows the total germ counts before and after the application of BDCT, and the results showed no significant difference ($p > 0.05$). In addition, no bacterial colony adhesion was found on BDCT (Figure S5a, Supporting Information) after interacting with guinea pig’s skin. We also used raw CT as the control, which really adhered bacterial colonies after being removed from this animal testing (Figure S5b, Supporting Information). These contrast experiments illustrated the value of BDCT and BDCT did not affect the species and amount of skin flora after contact with the skin.

Skin microbiome can significantly affect the body’s immunity.^[35] As reported, a significant drop of microorganisms was observed immediately after using some silver-containing antibacterial textile.^[17] Consequently, it would provide opportunities for the invasion of pathogenic microorganisms and the occurrence of diseases, due to the excessive use of strong bactericidal textiles.^[17] However, BDCT did not damage the protection barrier of skin flora, thus be able to maintain skin microecological balance. Meanwhile, BDCT acted as another protective barrier outside skin, reducing adhesion and invasion of foreign pathogen. These final results of the animal test are in agreement with above-mentioned bacterially and fungally antiadhesive performances of BDCT.

2.5. Skin Sensitization Test

In order to further ensure the safety of BDCT, skin irritation and sensitization test was conducted on healthy albino rabbits.^[20,36] Figure 4d shows the animal experimental model. BDCT and raw CT were applied directly to the back skin of the rabbits as illustrated in Figure S6 (Supporting Information) according to the ISO 10993.10-2010 standard.^[36] After 24, 48, and even 72 h, neither erythema nor edema was found (Figure 4e). As shown in Table S1 (Supporting Information), the skin erythema and edema score at (24 ± 2) , (48 ± 2) , and (72 ± 2) h after removing CT and BDCT for each animal were all 0. Thus, all the primary irritation score for each animal for BDCT and CT were 0, and the primary irritation index of BDCT is 0; just like raw CT (Table S2, Supporting Information). Based on the standard (Table S3, Supporting Information), the obtained index represented a negligible irritation. In addition, the hematoxylin and eosin (H&E) stained images of skin samples (Figure 4f) showed that no obvious histopathological abnormalities were observed after contacting with CT and BDCT. These phenomena of the absence of any dermal irritation also indicated that BDCT is structurally stable, where no BF or Aps small molecules release happened in the usage.

2.6. Microbially Antiadhesive Mechanism

Nowadays, mainly two mechanisms, microbial killing and microbial repelling, are widely developed for antimicrobial materials.^[37] The former may not only cause microbial resistance but also pose a threat to the environment and human safety.^[38,39] We designed a mild microbially antiadhesive method, which should belong to a microbial-repelling instead of a microbial-killing

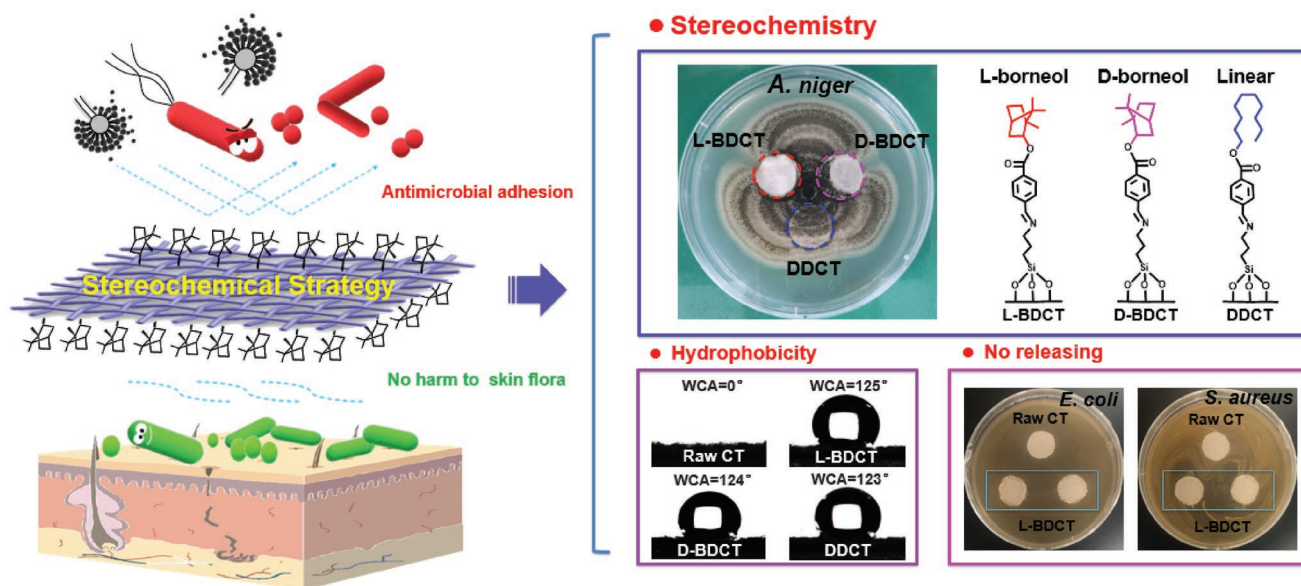


Figure 5. Schematic representation of microbially antiadhesive effect and mechanism of the BDCT.

method. It is a safe and harmonious antimicrobial strategy that isolates pathogens from the outside environment and does not harm the skin's inherent flora (Figure 5). In our opinion, it is mainly due to the unique stereochemical structure of borneol, a bicyclic monoterpene, which plays a crucial role in microbial antiadhesion. We have proved that L-borneol polyacrylate (PLBA) displayed better microbially antiadhesive performance than D-borneol polyacrylate (PDBA) in our previous research.^[25] Based on this finding, we used L-borneol to prepare BDCT in this study, which was regarded as L-BDCT in this chapter. To further prove the stereochemical strategy of microbial antiadhesion, we also prepared D-borneol-decorated CT (D-BDCT) by the same method. Figure S7 (Supporting Information) shows the ¹H nuclear magnetic resonance (¹H NMR) and ATR-FTIR characterizations for D-BF and D-BDCT. Figure S8 (Supporting Information) shows the circular dichroism (CD) spectra with strong mirror-image responses of L-BF and D-BF in the region of 220–260 nm. These results confirmed that the raw CT were decorated with stereoisomers of borneol. Then we tested its fungally antiadhesive performance against *A. niger* compared with L-BDCT. As shown in Figure 5 inset, after 6 d of incubation, colonized area of *A. niger* on L-BDCT and D-BDCT were 1 and 19%, respectively. This result demonstrated that L-BDCT displayed a better fungally antiadhesive effect than D-BDCT. In other words, stereochemistry is an effective strategy for microbial antiadhesion.

In addition, we used a linear 1-decanol structure to prepare a 1-decanol-decorated CT (DDCT) through the same method (Figures S9 and S10, Supporting Information), which was Schiff-base coupling of 1-decanol 4-formylbenzoate (DF) molecules onto the Aps-CT and tested its fungally antiadhesive performance. However, the linear DDCT did not show fungally antiadhesive property, showing the *A. niger* colonized area of 100% after 6 d of incubation (Figure 5 inset). This result indicated that the linear structure on the surface had no fungally antiadhesive property, though DDCT and BDCT have the same number of carbon atoms.

Furthermore, L-BDCT, D-BDCT, and DDCT showed the same hydrophobicity with the water contact angle (WCA) of 125°, 124°, and 123°, respectively (Figure 5 inset). Moreover, the inhibition zones of L-BDCT against *S. aureus* and *E. coli* were both zero (Figure 5 inset). That is, the L-BDCT did not release germicidal ingredients, ensuring the safety of L-BDCT to skin flora and no skin sensitization during usage. All these results demonstrated that the microbially antiadhesive activity was due to the influence of the surface bicyclic-stereochemistry of borneol instead of hydrophobicity. The interaction between textile and microorganisms is the key factor to answer this antiadhesion. The long linear alkyl chain could be a suitable handle with good affinity toward bacterial membrane, while the borneol may not have such affinity although having the same carbon number and contact angle result.

2.7. Durability and Usability

To further study the microbially antiadhesive durability, the bacterially and fungally antiadhesive performances of BDCT were evaluated after 10, 20, 30, 40, and 50 times of laundering according to FZ/T 73023-2006 standard method.^[20] After 50 times of laundering cycles, the log₁₀ reduction in bacterial adhesion count of *E. coli*, *P. aeruginosa*, *S. aureus*, and *S. epidermidis* on BDCT, compared with raw CT, were 1.23, 1.19, 1.56, and 1.54, respectively (Figure 6a). While the fungal colonized area of *A. niger* after 30 d of incubation on BDCT was only 4.6% which was considerably lower than that on raw CT (100%) (Figure 6b). Totally, with an increase of washing cycles from 0 to 50 times, the microbial antiadhesion performance of BDCT did not change much. These results demonstrated that the BDCT had durable microbially antiadhesive activities against general microbes.

The durability of BDCT is coming from the structural stability of hydrophobic Schiff-base binding. Big hydrophobic

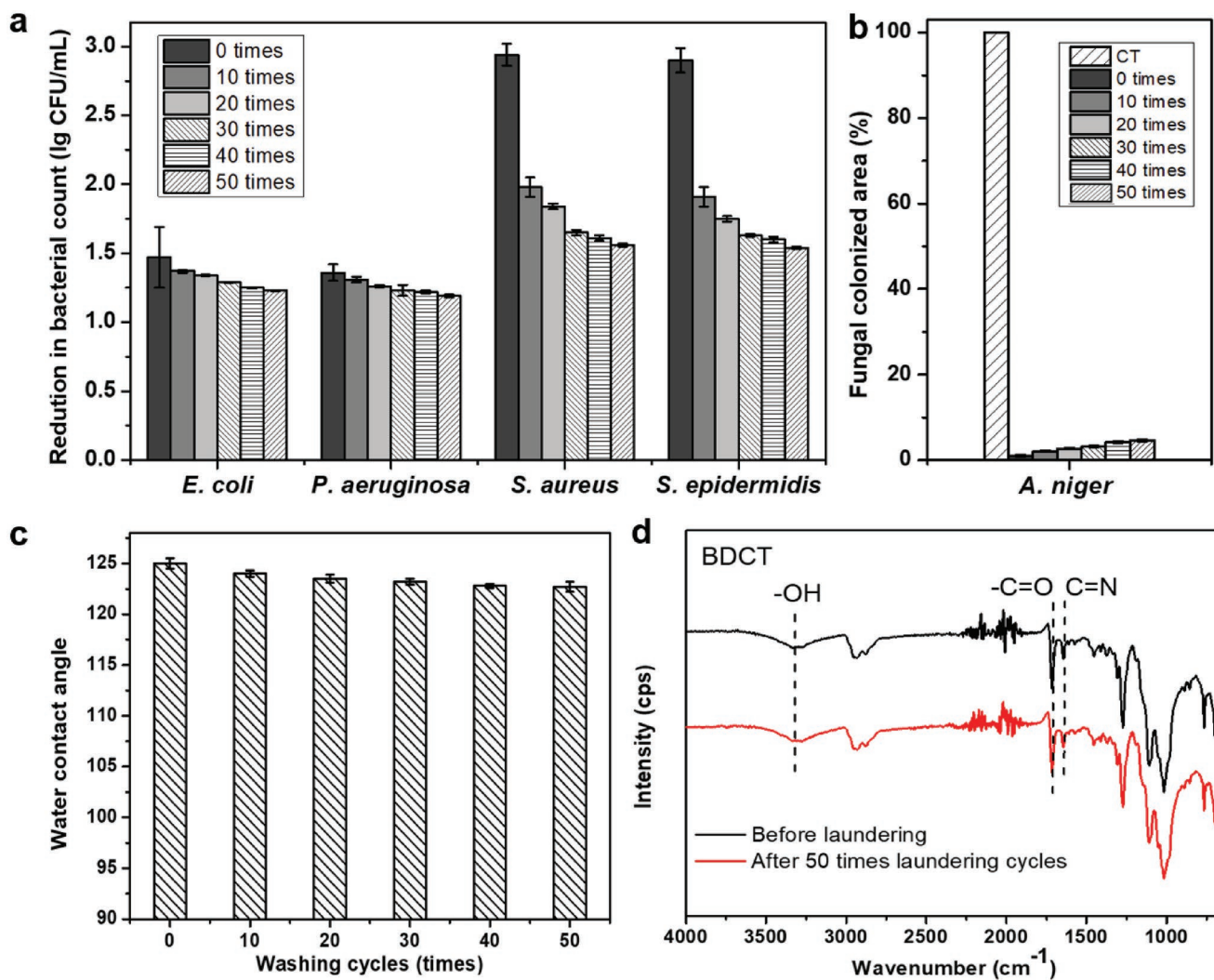


Figure 6. a) Log₁₀ reduction in bacterial adhesion count of *E. coli*, *P. aeruginosa*, *S. aureus*, and *S. epidermidis* on BDCT after 0, 10, 20, 30, 40, and 50 times of repetitive washing cycles. Data presented as mean ± SD, *n* = 3. b) Fungal colonized area of *A. niger* after 30 d of incubation on raw CT and BDCT after 0, 10, 20, 30, 40, and 50 times of repetitive washing cycles. Data presented as mean ± SD, *n* = 3. c) WCA of BDCT after 0, 10, 20, 30, 40, and 50 times of repetitive washing cycles. Data presented as mean ± SD, *n* = 3. d) ATR-FTIR survey spectra of BDCT before and after 50 times of repetitive washing cycles.

group could stabilize Schiff base even in acid conditions.^[29–31] The bicycle borneol group is a big hydrophobic group, thus providing a stable modification and durable antimicrobial capability. Evidence could be found by the inhibition zone test of BDCT (Figure 5). And, the hydrophobic property of BDCT was retained over a WCA of 122° after 50 repetitive washing cycles (Figure 6c). Besides, ATR-FTIR measurements further proved the structural stability of BDCT. As shown in Figure 6d, the similar ATR-FTIR spectra of BDCT before and after 50 laundering cycles suggested that there was no change in the molecular structures. The characteristic absorption peaks of Schiff base at 1720 cm⁻¹ (C=O vibration) and 1640 cm⁻¹ (C=N vibration) still exist. We further confirmed the Schiff-base stability of BDCT at the range of pH 3–11 (Figure S11, Supporting Information). Anyway, at least now we know that most detergents are alkaline (Table S4, Supporting Information). Hence, the Schiff-base of BDCT was strong enough to survive the detergent effect in laundering.

The properties for the usage of BDCT are also important. Though the appearance and whiteness did not show any changes (Figure 1b,b'), the mechanical properties of BDCT were improved with a certain degree compared with raw CT (Figure 7). The breaking strength increased from 295 to 332 N in weft direction and increased from 476 to 505 N in warp direction. As well, the breaking elongation was improved from 10.24 to 12.57% in weft direction and from 23.36 to 29.79% in warp direction. Thus, the BDCT displayed good usability due to the stable and uniform decoration.

3. Conclusion

In summary, we developed a novel BDCT with both bacterially and fungally antiadhesive properties and excellent laundering durability through a simple two-step decoration of borneol

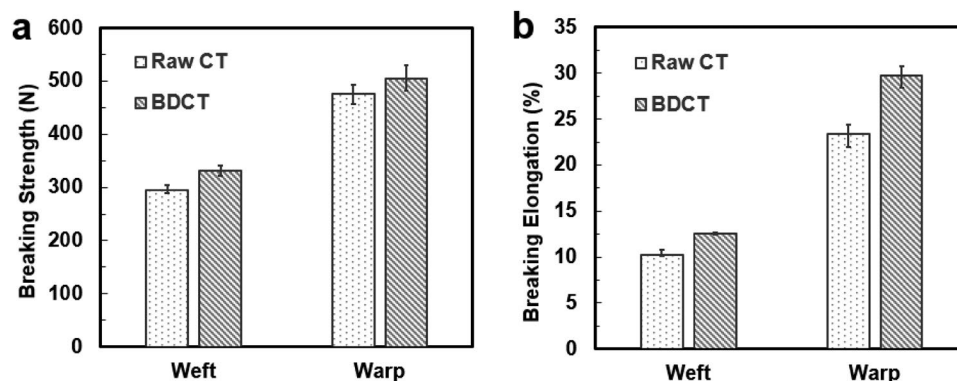


Figure 7. a) Breaking strength and b) breaking elongation of raw CT (control) and BDCT. Data presented as mean \pm SD, $n = 5$.

terminal groups on CT. The new functionalized CT exhibited prominent fungal antiadhesion against *M. racemosus*, *A. niger*, and *C. albicans* for more than 30 d. It also exhibited broad-spectrum bacterially antiadhesive activities against both Gram-negative and Gram-positive bacteria such as *E. coli*, *P. aeruginosa*, *S. aureus*, and *S. epidermidis*. The microbial antiadhesion performance was durable even after 50 times of accelerated laundering test. In-depth investigation demonstrated that the microbially antiadhesive activity was mainly due to the surface stereochemistry of borneol instead of hydrophobicity or others, though the hydrophobicity and mechanical properties of BDCT were improved.

Therefore, it is different from traditional microbial-killing strategy that usually causes damage to skin flora. BDCT was harmless to skin flora and conducive to maintain skin microecological balance. It also showed no skin stimulation, one reason might be no releasing of germicidal substances. Hence in the perspective of application, BDCT is meeting the frontier of antimicrobial CT, where beneficial skin flora should live in harmony with the functional CTs, as well as protecting us from potentially harmful microorganisms. Thus, BDCT-like materials would be of great significance in safeguarding beneficial microorganisms, utilizing in many industries, such as clothing, medical, and food packaging, and environmental or engineering domains, as well as to control the spread of unwanted microorganisms.

4. Experimental Section

Materials: 4-Formylbenzoic acid (97%), Aps (97%), and anhydrous tetrahydrofuran (THF, 99.5%) were purchased from J&K Scientific. 4-Dimethylaminopyridine (DMAP, 99%) and *N,N'*-dicyclohexylcarbodiimide (DCC, 99%) were purchased from Tokyo Chemical Industry (TCI). *L*-Borneol (97%) and *D*-borneol (97%) were purchased from Sigma-Aldrich. Malt extract agar, tryptone soy agar (TSA), and trypticase soy broth (TSB) were purchased from Aladdin. The BacLight live/dead kit (Molecular Probes) was purchased from Thermo Fisher Scientific. Other reagents were purchased from Sinopharm Chemical Reagent Co., Ltd, China. *E. coli* (ATCC 25922), *S. aureus* (ATCC 25923), *P. aeruginosa* (CICC 10351), *S. epidermidis* (CICC 1043), *M. racemosus* (CICC 3161), *A. niger* (CICC 41254), and *C. albicans* (CICC 32380) were obtained from the China Center of Industrial Culture Collection.

Synthesis of BF: 4-Formylbenzoic acid (1.45 g, 9.66 mmol), DMAP (0.15 g, 1.23 mmol), DCC (2.6 g, 12.60 mmol), and borneol

(1.00 g, 6.48 mmol) were added into 30 mL of THF with a calcium chloride drying tube. The reaction was maintained at room temperature for 12 h. Finally, the target product BF with a total yield over 95% was obtained by filtration, evaporation, and further purification with silica gel column chromatography (200–300 mesh; the eluents were petroleum ether:ethyl acetate = 10:1). ^1H NMR (JNM-ECA400, JEOL) and FTIR spectroscopy (IR Affinity-1, SHIMADZU) were used to confirm the chemical features of BF, and the results are shown in Figure S12 (Supporting Information).

Preparation of BDCT: First, a cleaned CT sample was soaked in a previously prepared solution of toluene containing Aps ($v/v = 10:1$). After this, the CT sample was washed with toluene to remove the excessive APS and then heated at 80 °C for 1 h to promote covalent bonding. Then CT modified with Aps was obtained after washing with toluene thoroughly, moving the unreacted Aps and impurities on the textile surface. After drying, CT modified with Aps was immersed into ethanol solution containing BF (0.01 g mL $^{-1}$) for 2 h at room temperature. Finally, the BDCT sample was washed with ethanol thoroughly to remove the residual BF and dried at room temperature.

Characterization and Measurement: SEM (JSM-7800F, JEOL) was used to observe the morphology of CT before and after decorating. ATR-FTIR (Perkin-Elmer Spectrum 100 spectrometer, Waltham, MA) was used to observe the surface chemical structure. XPS (Thermo Fisher Scientific, Waltham, MA) was used to detect the surface elemental composition. Tensile strength and elongation at break of textiles (the warp and weft direction) were determined with a testing machine (MTS systems Co., Ltd., Shanghai, China). WCA measurement was performed on a JC2000D3 (Zhongyi Kexin Technology Co., Ltd., Beijing, China) at room temperature. The whiteness of the textiles was measured by an SC-80C automatic chromometer (Kang Guang Instrument Co., Ltd., Beijing, China) and it was calculated under D65 illumination and CIE 1964 standard observer;^[40] each sample was measured at three different positions, with each reported value representing the means of five samples. The DG of the coating on BDCT was measured by gravimetric method and calculated as follows^[6]

$$DG = (W_g - W_0) / W_0 \times 100\% \quad (1)$$

where W_0 is the weight of the raw CT and W_g is the weight of BDCT. CD spectrometer (Bio-Logic MOS-500, France) was used to characterize BF molecular chirality.

Bacterial Adhesion Tests: The bacteria were incubated in fresh TSB medium at 37 °C with a shaking incubator overnight (200 rpm). The bacterial suspension was then diluted to a concentration of 10 7 CFU mL $^{-1}$ by sterile normal saline for later use.

First, BDCT and raw control CT were incubated with 3 mL of bacterial suspension (10 7 CFU mL $^{-1}$) at 37 °C for 4 h. Second, after rinsing gently with sterile normal saline three times, bacteria strongly adhered on the surface of BDCT and raw control CT were dispersed into 3 mL of sterile normal saline by using an ultrasonic cleaner. Finally, a 100 μL dispersion

was coated on TSA medium and further cultured for 24 h at 37 °C. After counting the number of colonies, the number of adhered bacteria was calculated by multiplying the number of colonies by the dilution factor. Each experiment was carried out three times and the significant differences of CT and BDCT for each bacteria type were obtained by statistical analysis. In addition, calculate the \log_{10} reduction in bacterial adhesion count of BDCT. The data were presented as mean \pm standard deviation (SD).

After ultrasonic cleaning of raw CT and BDCT, the obtained bacterial suspension was stained using the BacLight live/dead kit (Molecular Probes, Eugene, OR). Added 1.5 μL of 3.34×10^{-3} M SYTO9 stain and 1.5 μL of 30×10^{-3} M PI stain to 1 mL of the bacterial suspension mentioned above. The SYTO9 stain can be internalized into cell cytoplasm regardless of membrane condition whereas PI can traverse disrupted cytoplasmic membranes only. Live bacteria were stained with SYTO9 to produce green fluorescence, and dead bacteria were stained with PI to produce red fluorescence. The stain-treated bacteria suspension was incubated in the dark for 15 min followed by washing in saline solution and centrifugation. Resuspended stained bacteria were spotted (10 μL) on a microscopic slide and visualized under a fluorescence microscope with a cover slip.

Fungal Adhesion Experiments: *M. racemosus*, *A. niger*, and *C. albicans* were used here. The fungus was cultivated on malt extract agar medium and incubated at 30 °C for 7 d according to the streak-plate method. Following incubation, fungal cells were eluted and collected by 5 mL of 0.9% saline, and then shocked by a vortex mixer until the cells were homogeneously dispersed. The concentration of spore suspension for each fungal species was determined with a hemocytometer and adjusted to 10^8 spores mL^{-1} for the antifungal experiments. Circular samples with 15.0 ± 0.1 mm in diameter made from BDCT, raw CT, and Aps-CT were cut and fixed onto malt extract agar medium. Then, 10 μL of fungal suspension was dropped in the center of the plate, ensuring the same distance to the test samples. The plate was thermostatically cultured at 30 °C in a mold incubator. In this condition, fungi could grow and expand from the medium center to the samples. The growth phenomenon of the fungi at different periods was observed and recorded with a camera. The antiadhesive properties after four repeated challenges were conducted by repeatedly challenging the same BDCT with *A. niger* every 4 d of intervals.

SEM (S-4700 Hitachi) was used to observe the morphology of fungal cells on raw CT and BDCT surface. After 30 d incubation, samples mentioned above were immobilized with 2.5% glutaraldehyde for 2 h at 4 °C. Then, fungal cells were dehydrated by 50, 60, 70, 80, 90, and 100% ethanol for 20 min, respectively. Finally, the samples were vacuum-dried for 12 h prior to the SEM observation.

Skin Flora Evaluation: 30 healthy albino guinea pigs, 15 males and 15 females (weight of 250–300 g, Beijing Vital River Laboratory Animal Technology Co., Ltd., Beijing, China) were treated and cared for in accordance with the National Research Council's Guide for the care and use of laboratory animals. They were shaved on both sides of back to ensure all textiles had a close fit with the sample before the experiment. All the experiment appliances were sterilized by autoclave and the samples were sterilized by UV for 0.5 h. A standard scrub method developed by Williamson and Kligman^[41] was used and slightly optimized to collect the skin microflora. First, the microbes were taken from guinea pigs' skin with cotton swabs after wetting in sterile saline, and then 2.5 cm \times 2.5 cm BDCT was directly applied to the shaved region of guinea pigs' back. After 6 h, the dressing was removed and the microbes from the region were taken using the same method. After sampling, the cotton swabs were placed in 3 mL of sterile saline and washed with an ultrasonic wave for 10 min. 100 μL of each wash water was sampled to disperse uniformly on the surface of TSA plates and incubated at 37 °C. After 24 h of incubation, the number of colony forming units was determined and recorded. The analytical data were expressed as CFU cm^{-2} of guinea pig skin. The bacteria detected from the skin before and after contacting BDCT were identified according to their 16S rDNA sequence analysis.

Skin Sensitization Test: Three healthy male albino rabbits weighing 2.0–2.5 kg were purchased from the Beijing Fuhao Experimental Animal

Breeding Center (Beijing, China) and were treated and cared for in accordance with the National Research Council's Guide for the care and use of laboratory animals. They were shaved on the back and then two 2.5 cm \times 2.5 cm BDCT and two untreated control CT were directly applied to the back skin. After 6 h, the dressings were removed, the positions of the dressings were marked with pen, and the appearances of each position were recorded at (1 ± 1) , (24 ± 2) , (48 ± 2) , and (72 ± 2) h after removing the samples. All erythema score and edema score at (24 ± 2) , (48 ± 2) , and (72 ± 2) h for BDCT and raw CT for each animal were scored according to the ISO 10993.10-2010 standard was showed in Table S5 (Supporting Information). The primary irritation score for an animal was calculated by dividing the sum of all the scores by 6 (two test sites, three time-points). The primary irritation index was obtained by taking the average of three rabbits primary irritation score. Primary irritation index categories in rabbit according to the ISO 10993.10-2010 standard are shown in Table S3 (Supporting Information). Meanwhile, the skin tissue samples after contacting with CT and BDCT were sliced and stained with H&E for histopathological changes evaluated by microscopy.

Microbially Antiadhesive Durability Test: In a simplified washing cycle, 10 g CT sample was first washed for 25 min in the washing machine (Haier XQBM33-1699) with 6 g common washing agent and 30 L water at 40 ± 3 °C. Thereafter, the sample was rinsed two times, each of which was washed for 2 min and dehydrated for 1 min. The above steps were equivalent to five times standard launderings according to FZ/T 73023-2006 standard and then, repeated for 2, 4, 6, 8, and 10 cycles to the predetermined washing time. \log_{10} reduction in bacterial adhesion count of *E. coli*, *P. aeruginosa*, *S. aureus*, and *S. epidermidis*, fungal colonized area of *A. niger* after 30 d of incubation and WCA of the treated BDCT were measured after 10, 20, 30, 40, and 50 times washing cycles. Each experiment was carried out three times and the data were presented as mean \pm SD. The chemical structure of the BDCT before and after 50 repetitive washing cycles was measured by ATR-FTIR spectroscopy analysis. The inhibition zones of raw CT and BDCT against *S. aureus* and *E. coli* were determined by diffusion method on agar plate according to GB/T 31713-2015 standard method.

pH Stability Measurement: The pH stability experiments were carried out in solutions at different pH values ranging from pH 3 to pH 11, where NaOH or HCl was used to modulate the pH value. The BDCT samples were incubated in buffers with stirring at 25 °C for 0.5 h. Afterward, they were washed with ethanol and deionized water three times, respectively. Finally, the BDCT samples were dried at room temperature and characterized by ATR-FTIR.

Statistical Analysis: SPSS 16.0 was used for statistical analysis in this study. All the quantitative data were presented as mean \pm SD for bacterially antiadhesive experiments ($n = 3$), microbially antiadhesive durability test ($n = 3$), and skin flora experiments ($n = 30$). After normal distribution was confirmed, the two-tailed Student's *t*-tests were performed to evaluate the bacterial adhesion number on CT and BDCT, and the total germ counts of guinea pig skin before and after applying BDCT. *p*-values < 0.05 were taken to be statistically significant.

Supporting Information

Supporting Information is available from the Wiley Online Library or from the author.

Acknowledgements

The authors thank the National Natural Science Foundation of China (21574008), the Fundamental Research Funds for the Central Universities (PYBZ1806 and BHYC1705B) of China, and National Institute of Health (NIH, A1110924) for their financial support. X.W. also gratefully acknowledges China Scholarship Council for their financial support on a Visiting Scholar Program (No. 201706885008).

Conflict of Interest

The authors declare no conflict of interest.

Keywords

borneol, cotton textiles, microbial antiadhesion, skin flora, surface decoration

Received: February 20, 2019

Revised: May 23, 2019

Published online:

- [1] Y. Y. Zhang, Q. B. Xu, F. Y. Fu, X. D. Liu, *Cellulose* **2016**, *23*, 2791.
- [2] S. G. Chen, L. J. Yuan, Q. Q. Li, J. N. Li, X. L. Zhu, Y. G. Jiang, O. Sha, X. H. Yang, J. H. Xin, J. X. Wang, F. J. Stadler, P. Huang, *Small* **2016**, *12*, 3516.
- [3] B. Simoncic, B. Tomsic, *Text. Res. J.* **2010**, *80*, 1721.
- [4] C. Q. Yuan, M. Bide, M. Phaneuf, W. Quist, F. Logerfo, *AATCC Rev.* **2001**, *1*, 35.
- [5] D. Štular, I. Jerman, I. Naglič, B. Simončič, B. Tomšič, *Carbohydr. Polym.* **2017**, *159*, 161.
- [6] D. G. Gao, Y. J. Li, B. Lyu, L. H. Lyu, S. W. Chen, J. Z. Ma, *Carbohydr. Polym.* **2019**, *204*, 161.
- [7] P. Elsner, *Curr. Probl. Dermatol.* **2006**, *33*, 35.
- [8] Y. Y. Liu, K. K. Ma, R. Li, X. L. Ren, T. S. Huang, *Cellulose* **2013**, *20*, 3123.
- [9] B. Ocepek, B. Boh, B. Šumiga, P. F. Tavčar, *Color. Technol.* **2012**, *128*, 95.
- [10] X. R. Fu, Y. Shen, X. Jiang, D. Huang, Y. Y. Yan, *Carbohydr. Polym.* **2011**, *85*, 221.
- [11] C. E. Zhou, C. W. Kan, *Cellulose* **2014**, *21*, 2951.
- [12] Y. Gao, R. Cranston, *Text. Res. J.* **2008**, *78*, 60.
- [13] S. P. Yazdankhah, A. A. Scheie, E. A. Høiby, B. T. Lunestad, E. Heir, T. Ø. Fotland, K. Naterstad, H. Kruse, *Microb. Drug Resist.* **2006**, *12*, 83.
- [14] D. E. Latch, J. L. Packer, W. A. Arnold, K. McNeill, *J. Photochem. Photobiol., A* **2003**, *158*, 63.
- [15] P. Canosa, I. Rodríguez, E. Rubí, R. Cela, *Anal. Chem.* **2007**, *79*, 1675.
- [16] H. T. Yang, G. F. Li, J. W. Stansbury, X. Q. Zhu, X. Wang, J. Nie, *ACS Appl. Mater. Interfaces* **2016**, *8*, 28047.
- [17] D. Hofer, T. R. Hammer, *ISRN Dermatol.* **2011**, *2*, 369603.
- [18] A. Bouslimani, C. Porto, C. M. Rath, M. X. Wang, Y. R. Guo, A. Gonzalez, D. Berg-Lyon, G. Ackermann, G. J. M. Christensen, T. Nakatsuji, L. J. Zhang, A. W. Borkowski, M. J. Meehan, K. Dorrestein, R. L. Gallo, N. Bandeira, R. Knight, T. Alexandrov, P. C. Dorrestein, *Proc. Natl. Acad. Sci. USA* **2015**, *112*, E2120.
- [19] S. B. Zhang, X. H. Yang, B. Tang, L. J. Yuan, K. Wang, X. Y. Liu, X. L. Zhu, J. A. Li, Z. C. Ge, S. G. Chen, *Chem. Eng. J.* **2018**, *336*, 123.
- [20] S. G. Chen, S. J. Chen, S. Jiang, M. L. Xiong, J. X. Luo, J. N. Tang, Z. C. Ge, *ACS Appl. Mater. Interfaces* **2011**, *3*, 1154.
- [21] J. Lin, X. Chen, C. Y. Chen, J. T. Hu, C. L. Zhou, X. F. Cai, W. Wang, C. Zheng, P. P. Zhang, J. Cheng, Z. H. Guo, H. Liu, *ACS Appl. Mater. Interfaces* **2018**, *10*, 6124.
- [22] P. M. Sivakumar, V. Prabhawathi, R. Neelakandan, M. Doble, *Biomater. Sci.* **2014**, *2*, 990.
- [23] X. Wang, H. Gan, T. L. Sun, B. L. Su, H. Fuchs, D. Vestweber, S. Butz, *Soft Matter* **2010**, *6*, 3851.
- [24] X. Wang, H. Gan, M. X. Zhang, T. L. Sun, *Langmuir* **2012**, *28*, 2791.
- [25] L. Q. Luo, G. F. Li, D. Luan, Q. P. Yuan, Y. Wei, X. Wang, *ACS Appl. Mater. Interfaces* **2014**, *6*, 19371.
- [26] X. L. Sun, Z. Y. Qian, L. Q. Luo, Q. P. Yuan, X. M. Guo, L. Tao, Y. Wei, X. Wang, *ACS Appl. Mater. Interfaces* **2016**, *8*, 28522.
- [27] B. Shi, D. Luan, S. H. Wang, L. Y. Zhao, L. Tao, Q. P. Yuan, X. Wang, *RSC Adv.* **2015**, *5*, 51947.
- [28] J. Q. Xu, Y. J. Bai, M. J. Wan, Y. H. Liu, L. Tao, X. Wang, *Polymers* **2018**, *10*, 448.
- [29] J. Mao, Y. Li, T. Wu, C. H. Yuan, B. R. Zeng, Y. T. Xu, L. Z. Dai, *ACS Appl. Mater. Interfaces* **2016**, *8*, 17109.
- [30] N. A. Negm, Y. M. Elkholy, M. K. Zahran, S. M. Tawfik, *Corros. Sci.* **2010**, *52*, 3523.
- [31] Y. N. Fu, Y. S. Li, G. F. Li, L. Yang, Q. P. Yuan, L. Tao, X. Wang, *Biomacromolecules* **2017**, *18*, 2195.
- [32] Y. Z. Li, B. J. Wang, X. F. Sui, R. Y. Xie, H. Xu, L. B. Zhang, Y. Zhong, Z. P. Mao, *Appl. Surf. Sci.* **2018**, *435*, 1337.
- [33] Y. E. Chen, M. A. Fischbach, Y. Belkaid, *Nature* **2018**, *553*, 427.
- [34] E. Abd, S. A. Yousef, M. N. Pastore, K. Telaprolu, Y. H. Mohammed, S. Namjoshi, J. E. Grice, M. S. Roberts, *Clin. Pharmacol.: Adv. Appl.* **2016**, *8*, 163.
- [35] S. Naik, N. Bouladoux, J. L. Linehan, S. J. Han, O. J. Harrison, C. Wilhelm, S. Conlan, S. Himmelfarb, A. L. Byrd, C. Deming, M. Quinones, J. M. Brenchley, H. H. Kong, R. Tussiwand, K. M. Murphy, M. Merad, J. A. Segre, Y. Belkaid, *Nature* **2015**, *520*, 104.
- [36] M. Yu, Z. Q. Wang, M. Lv, R. Z. Hao, R. T. Zhao, L. H. Qi, S. M. Liu, C. H. Yu, B. W. Zhang, C. H. Fan, J. Y. Li, *ACS Appl. Mater. Interfaces* **2016**, *8*, 19866.
- [37] X. K. Ding, S. Duan, X. J. Ding, R. H. Liu, F. J. Xu, *Adv. Funct. Mater.* **2018**, *28*, 1802140.
- [38] Z. L. Fei, B. J. Liu, M. F. Zhu, W. Wang, D. Yu, *Cellulose* **2018**, *25*, 3179.
- [39] M. S. Hassan, H. E. Ali, N. M. Ali, *J. Vinyl Addit. Technol.* **2017**, *23*, E34.
- [40] R. Jafari, S. H. Amirshahi, *Text. Res. J.* **2007**, *77*, 756.
- [41] P. Williamson, A. M. Kligman, *J. Am. Acad. Dermatol.* **1965**, *45*, 498.